NeuroImage 136 (2016) 139–148

Contents lists available at ScienceDirect

NeuroImage

journal homepage: www.elsevier.com/locate/ynimg

Frontal preparatory neural oscillations associated with cognitive control: A developmental study comparing young adults and adolescents

Kai Hwang [a,b,c,d,*], Avniel S. Ghuman [b,d,e], Dara S. Manoach [f,g], Stephanie R. Jones [h], Beatriz Luna [b,c,d]

[a] Helen Wills Neuroscience Institute, University of California Berkeley, Berkeley, CA, United States
[b] Department of Psychiatry, University of Pittsburgh, Pittsburgh, PA, United States
[c] Department of Psychology, University of Pittsburgh, Pittsburgh, PA, United States
[d] Center for the Neural Basis of Cognition, Carnegie Mellon University and University of Pittsburgh, Pittsburgh, PA, United States
[e] Department of Neurological Surgery, University of Pittsburgh, Pittsburgh, PA, United States
[f] Department of Psychiatry, Massachusetts General Hospital, Harvard Medical School, Boston, MA, United States
[g] Athinoula A. Martinos Center for Biomedical Imaging, Charlestown, MA, United States
[h] Department of Neuroscience, Brown University, Providence, RI, United States

ARTICLE INFO

Article history:
Received 14 December 2015
Revised 24 March 2016
Accepted 5 May 2016
Available online 10 May 2016

Keywords:
Adolescence
Antisaccade
Frontal cortex
Inhibitory control
Neural oscillations

ABSTRACT

Functional magnetic resonance imaging (fMRI) studies suggest that age-related changes in the frontal cortex may underlie developmental improvements in cognitive control. In the present study we used magnetoencephalography (MEG) to identify frontal oscillatory neurodynamics that support age-related improvements in cognitive control during adolescence. We characterized the differences in neural oscillations in adolescents and adults during the preparation to suppress a prepotent saccade (antisaccade trials—AS) compared to preparing to generate a more automatic saccade (prosaccade trials—PS). We found that for adults, AS were associated with increased beta-band (16–38 Hz) power in the dorsal lateral prefrontal cortex (DLPFC), enhanced alpha- to low beta-band (10–18 Hz) power in the frontal eye field (FEF) that predicted performance, and increased cross-frequency alpha-beta (10–26 Hz) amplitude coupling between the DLPFC and the FEF. Developmental comparisons between adults and adolescents revealed similar engagement of DLPFC beta-band power but weaker FEF alpha-band power, and lower cross-frequency coupling between the DLPFC and the FEF in adolescents. These results suggest that lateral prefrontal neural activity associated with cognitive control is adult-like by adolescence; the development of cognitive control from adolescence to adulthood is instead associated with increases in frontal connectivity and strengthening of inhibition signaling for suppressing task-incompatible processes.

Introduction

The ability to generate a task compatible response while suppressing prepotent and incompatible responses is a core component of cognitive control (Aron, 2007; Garavan et al., 2002; Ridderinkhof et al., 2004). This may be achieved through proactive, preparatory control processes (Aron, 2011; Braver, 2012) that modulate response related neural activities in preparation for an action (Cai et al., 2011; Connolly et al., 2002; DeSouza et al., 2003; Lavallee et al., 2014; Sacchet et al., 2015; Worden et al., 2000). Cognitive control has a protracted development through adolescence, in parallel with several circuit and systems level maturational processes (Luna et al., 2015). Initial developmental fMRI studies using tasks that require response inhibition show disparate results often implicating immaturity in prefrontal cortical systems (Bunge et al., 2002; Durston et al., 2002; Rubia et al., 2006, 2007; Velanova et al., 2009). Thus probing the neurodevelopmental differences in frontal preparatory processes is critical for understanding limitations in cognitive control during adolescence.

The antisaccade task (AS), which requires one to suppress a prepotent visually guided saccade in favor of a voluntary guided saccade to the opposite location, has been used to investigate the neural basis of preparatory cognitive control (Everling and Fischer, 1998). Non-human primate studies indicate that neural activities in oculomotor regions such as the frontal eye field (FEF), the supplementary eye field, and the superior colliculus (SC) during the preparatory period of the AS task predict correct versus incorrect AS task performance (Everling et al., 1998, 1999; Everling and Munoz, 2000; Schlag-Rey et al., 1997). Evidence indicates that top-down signaling modulates activity of saccade neurons in the FEF and the SC (Everling et al., 1998; Everling and Munoz, 2000), reducing the excitability of saccade neurons and/or adjusting the saccade generation threshold (Munoz and Everling, 2004). One possible source of this top-down signal is the prefrontal cortex (PFC), where the task-rule (AS vs. PS) information is actively maintained (Buschman et al., 2012; Johnston and Everling, 2006b).

* Corresponding author at: 132 Barker Hall, University of California Berkeley, California, CA 94720, United States.
E-mail address: kai.hwang@berkeley.edu (K. Hwang).

http://dx.doi.org/10.1016/j.neuroimage.2016.05.017
1053-8119/

AS performance improves through adolescence as reflected in an increased rate of correct inhibitory responses (Alahyane et al., 2014; Fischer et al., 1997; Fukushima et al., 2000; Klein and Foerster, 2001; Kramer et al., 2005; Luna et al., 2004; Munoz et al., 1998). Our developmental fMRI studies using the AS suggest that increased engagement of frontal regions such as the FEF and ACC (Ordaz et al., 2013; Velanova et al., 2008), as well as strengthening of prefrontal top-down connectivity (Hwang et al., 2010), may support developmental improvements in AS performance (Hwang and Luna, 2012). However, in addition to developmental changes in activation magnitudes, we do not understand the differences in the temporal and spectral dynamics of neuronal activities that may underlie developmental changes in frontal processes, limiting our ability to probe neurobiological mechanisms.

Magnetoencephalography (MEG), which measures electrophysiological activities generated by neuronal dynamics at a high temporal resolution, allows us to probe neuronal dynamics underlying the *preparatory* processes critical for AS performance and how preparatory activities change with age. MEG characterizes synchronous neural oscillations that have been hypothesized to support the coordination of brain functions for cognitive control (Buschman et al., 2012; Canolty and Knight, 2010; Cohen, 2011; Fries, 2015; Sacchet et al., 2015). Particularly relevant to cognitive control are beta and alpha rhythms. Beta rhythms (19–40 Hz; Buschman et al., 2012) can be generated by glutamatergic excitation in the deep layers of cortical columns (Roopun et al., 2010) or via top down inputs to supragranular layers that activate deep layer pyramidal neurons through their distal dendrites (Jones et al., 2009), which in turn send efferents to subcortical and other cortical regions (Douglas and Martin, 2004), supporting top-down control of sensory and motor processes for goal-directed behaviors (Buschman et al., 2012; Buschman and Miller, 2007; Gross et al., 2006; Picazio et al., 2014; Saalmann et al., 2007; Swann et al., 2009). Alpha-band activity (6–16 Hz; Buschman et al., 2012) has been found to reflect functional inhibition (8–14 Hz; Jensen and Mazaheri, 2010; Jones et al., 2010; Klimesch et al., 2007), as it is negatively correlated with neural spiking rate (Haegens et al., 2011) and increases during suppression of attention (Belyusar et al., 2013; Handel et al., 2011; Thut et al., 2006; Worden et al., 2000). A recent study shows alpha band synchrony between pre-frontal and primary sensory cortex increases in non-attended representation soon after an attentional cue as a means to inhibit distracting sensory stimuli, while beta band synchrony increases closer to stimulus processing, presumably to facilitate accurate sensory processing and motor response (Sacchet et al., 2015). Therefore, proactive cognitive control may be achieved by beta-band oscillations for top-down processes and alpha-band activity for suppressing task-incompatible processes.

In our initial MEG AS study (Hwang et al., 2014) on adult subjects, we found that beta-band power in the DLPFC and alpha-band power in the FEF during the preparatory period increased for the AS task. Further, trial-by-trial prestimulus FEF alpha-band power was positively correlated with successful saccadic inhibition. Compared to the PS task, the AS task enhanced cross-frequency amplitude coupling between beta-band activity in the DLPFC and alpha-band activity in the FEF. These results suggest that frontal task-related oscillatory neurodynamics reflect top-down control signaling (DLPFC beta-band activity), functional inhibition of saccade-related neural activity (FEF alpha-band activity), and inter-regional coordination of task-control signal communication (cross-frequency coupling between the DLPFC and the FEF).

Oscillatory neural activities undergo significant changes during adolescence (Uhlhaas et al., 2009, 2010) and aging (Ziegler et al., 2010). Therefore a better understanding of alpha-band and beta-band oscillatory dynamics could provide important insights into how the PFC, FEF, and its interactions support AS task performance through adolescence. In the present study, we examined differences between adults and adolescents in beta-band activity, alpha-band activity, and beta-alpha coupling to identify frontal neural processes specific to age-related improvements in cognitive control. Given our earlier fMRI results (Hwang et al., 2010; Ordaz et al., 2013), we predicted that adolescents would demonstrate adult level beta-band oscillatory activity in DLPFC but immature FEF alpha-band activity, and weaker cross-frequency coupling between FEF and DLPFC.

Methods

Participants

We recruited 48 healthy volunteers with no history of psychiatric or neurological illness in either themselves or a first-degree relative. Of the 26 adults and 22 adolescents, we report data from 20 adults (10 male) aged 20 to 30 years ($M = 26.11$ years, $SD = 3.41$) and 17 adolescents (8 male) aged 14 to 16 years ($M = 15.74$ years, $SD = 0.94$). Data from 11 participants were excluded due to the following reasons: two adults and one adolescent because of MEG sensor noise that could not be removed, one adult because of excessive eye blinks, three adults and three adolescents because of an insufficient number of noise-free trials, and one adolescent because of a history of psychiatric disorder discovered after completing the experiment. The study was approved by the University of Pittsburgh Institutional Review Board, and all participants or their legal guardians gave written informed consent. Subjects were compensated for their participation. Findings from the adult participants were reported in our previous publication (Hwang et al., 2014).

Behavioral paradigm

Participants performed a total of 210 AS and 210 PS trials distributed across eight MEG runs. AS and PS trials were presented in blocks within each run to minimize task-switching effects known to alter behavioral performance and neural activity (Akaishi et al., 2010; Lee et al., 2010). The sequence of AS and PS blocks was pseudo-randomized within each run to ensure that the same task block did not repeat more than once. Each run included 10 or 11 task blocks, with five trials per block. A short resting block was inserted between task blocks. Each trial started with a preparatory period where an instructional cue ("cue") was presented for 1.5 s. A red "x" fixation in AS trials instructed subjects to look to the opposite location of the target, while a green "x" fixation instructed subjects to make an eye movement to the target. The preparatory period was followed by a "response period," in which the visual stimulus ("target") was presented for 1.5 s. The target was a solid yellow circle (size ~1°, luminance 42.22 cd/m^2), presented on the horizontal meridian at one of four unpredictable eccentricities ($\pm 6.3°$ and $\pm 10.6°$ from center fixation). A 1.2- to 1.6-s jittered white fixation mark was presented between trials. During data acquisition, visual stimuli were projected on a screen located one meter in front of the participant.

Crucial to this paradigm is that the target location is not revealed during the preparatory period to prevent the planning of a determined saccade. Therefore, by comparing preparatory activity between AS and PS trials, we could identify neurodynamics specific to proactive control processes, independent of motor signals associated with saccade execution. Our analyses focused on the preparatory period (starting 1.5 s before target onset), as previous non-human primate electrophysiology studies indicate that neural activity during the preparatory period is predictive of AS task performance (Everling et al., 1999; Everling and Munoz, 2000).

Data acquisition

All MEG data were acquired using an Elekta Neuromag VectorView MEG system (Elekta Oy, Helsinki, Finland) comprising 306 sensors arranged in triplets of two orthogonal planar gradiometers and one magnetometer. MEG data were acquired continuously with a sampling rate of 1000 Hz in a three-layer magnetically shielded room. We measured

head position relative to the MEG sensors throughout the recording period, and then used these head position estimates for off-line head movement correction. To monitor saccades and eye blinks, we used two bipolar electrode pairs to record vertical and horizontal electrooculogram (EOG). At the beginning of each participant's MEG session, we collected EOG calibration data to convert EOG voltage changes into saccade directions and amplitudes. Calibrated EOG data were then scored offline with the following criteria: saccades were identified as horizontal eye movements with velocities exceeding 40° per second, with minimum amplitudes of 3°. Fast express saccades can involve distinct subcortical mechanisms that MEG lacks the sensitivity to detect (Schiller et al., 1987); therefore, we excluded trials with both anticipatory and express saccades with initial saccade latencies faster than 130 ms. Accuracy was determined by comparing the location of the stimulus target and the required saccade direction. Structural MRI data were collected with a Siemens 3T Tim Trio system scanner to provide anatomical constraints for MEG source localization. A magnetization-prepared rapid acquisition with gradient echo (MP-RAGE) sequence was used with the following parameters: TR = 2100 ms, TI = 1050 ms, TE = 3.43 ms, 8° flip angle, 256x256x192 acquisition matrices, FOV = 256 mm, and 1 mm isotropic voxels.

MEG data preprocessing and trial selection

MEG sensor data were first inspected for flat or noisy channels, and then preprocessed using the temporal signal space separation (TSSS) method (Taulu and Hari, 2009; Taulu et al., 2004) to reduce noise and artifacts. TSSS reduces environmental magnetic artifacts and performs head movement compensation by aligning sensor-level data to a common reference (Nenonen et al., 2012). Cardiac artifacts, eye blinks, and saccade artifacts were then removed using an independent component analysis-based procedure. MEG sensor data were decomposed into independent components (ICs) using EEGLAB (Delorme and Makeig, 2004) algorithms implemented in the Fieldtrip software suite (Oostenveld et al., 2011). Each IC was then correlated with ECG and EOG recordings. An IC was designated as an artifact if the absolute value of the correlation was three standard deviations higher than the mean of all correlations. The "clean" ICs were then projected back to the sensor space for manual inspection.

To mitigate the effects of head motion on data quality, we adopted a conservative approach and rejected trials with sensor displacement greater than 1 mm. Low-amplitude, high-frequency sinusoidal continuous currents (>300 Hz) were fed to the four head-position-indicator coils positioned on the subject's head throughout MEG data recording. This allowed us to determine the position and orientation of the head with respect to the sensor array at 200-ms intervals throughout the scan (Nenonen et al., 2012). The amount of head motion was then estimated by calculating the frame-by-frame sensor displacement relative to the head position (Wehner et al., 2008). If at any time during the trial the displacement of MEG sensors was greater than 1 mm, the trial was rejected from all future analyses. Trials with saccades that occurred during the preparatory period or pretrial baseline were excluded, as were trials with gradiometer peak-to-peak amplitudes exceeding 3000 fT/cm or magnetometer peak-to-peak amplitudes exceeding 10 pT.

To maintain a constant signal-to-noise ratio (SNR) across conditions and age groups and prevent bias in estimating effects (Gross et al., 2013), we further fixed the number of trials per condition per participant at 47 correctly performed and noise-free trials (47 AS + 47 PS trials). We determined this number by calculating the lowest number of noise-free and correctly performed AS trials across all participants. For participants who had more than 47 usable trials, we selected trials randomly. For the logistic regression analyses, all correct and incorrect AS trials that were free of artifacts were included in the analyses (adults: mean ± *SD* = 151 ± 20 trials; adolescents: mean ± *SD* = 139 ± 13 trials). For all other analyses, we used only the selected 47 correct trials.

Source activity estimation and region of interest analyses

Single-trial MEG sensor data were projected from the sensors on to the cortical surface using the minimum-norm estimates (MNE) software (Gramfort et al., 2014). First, each participant's native cortical surface was reconstructed using Freesurfer (Dale et al., 1999; Fischl et al., 1999). After surface reconstruction, approximately 3000 dipoles with 7-mm spacing were placed on the gray/white matter boundary for each hemisphere. A forward solution was then calculated using a single compartment boundary-element model (Hamalainen and Sarvas, 1989). A noise covariance matrix was calculated from 700 to 400 ms before task cue presentation (during the inter-trial intervals) of trials that were free of artifacts. The noise covariance matrix and the forward solution were then combined to create a linear inverse operator (Dale et al., 2000) to project single-trial MEG sensor data to the cortical surface.

Regions of interest (ROIs) were defined within selected anatomical labels from Freesurfer's automatic parcellation of sulci and gyri based on each participant's structural MRI (Destrieux et al., 2010). We selected anatomical labels *a priori* based on their known involvement in inhibitory and oculomotor control. Specifically, the right DLPFC and the right ventral lateral prefrontal cortex were selected because prior studies demonstrated that these two regions are involved in motor inhibition and task-rule representation (Aron et al., 2004, 2014; Buschman et al., 2012; Hanes et al., 1998; N. Swann et al., 2012). Bilateral FEF and bilateral intraparietal sulcus (IPS) were selected because of their critical roles in saccade generation and preparatory processes (Brown et al., 2007; Hanes et al., 1998; Moon et al., 2007). We also included the primary visual cortex (V1) for control purposes. Because MEG is relatively insensitive to subcortical sources (Hamalainen et al., 2010), no subcortical ROIs were included. Similarly, the anterior cingulate cortex (ACC) and the supplementary eye field (SEF) were not included due to lower SNR compared to the lateral ROIs (Hwang et al., 2014). All ROIs were defined within individual subjects' native cortical surface. Anatomical labels used to define ROIs are shown in Fig. 1.

Within the selected anatomical regions, we selected the top 25% of dipoles where preparatory oscillatory activities showed robust change from baseline. The baseline window was defined as 700 to 400 ms prior to the cue presentation. Using complex Morelet wavelets (see below for details), we calculated oscillatory power across all frequencies (2–60 Hz) for every dipole within each label. For each frequency, a signal-to-noise estimate was then calculated by subtracting the mean baseline power from the mean power during the preparatory period, and dividing the difference by the variance of baseline power. The absolute values of *z*-scores were then averaged across frequencies, trials, and conditions (AS and PS) regardless of performance. This procedure is akin to deriving an omnibus test statistic for all conditions and frequencies, and it can be used to identify dipoles that show robust task-related oscillatory power. We then identified the dipoles with the top 25% maximum averaged *z*-score within each anatomical structure and defined

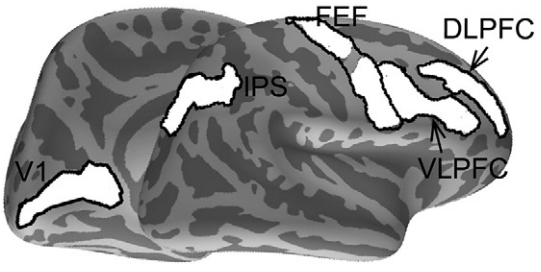

Fig. 1. Anatomical regions used to define ROIs. The following anatomical labels from freesurfer parcellation were used to constrain ROIs. FEF: superior and inferior part of the precentral sulcus. IPS: intraparietal sulcus. DLPFC: middle frontal sulcus. VLPFC: inferior frontal sulcus, opercular and triangular part of the inferior frontal gyrus. V1: the calcarine sulcus. Note that for each participant, ROIs were created in their respective native surface space, thus the exact dipole location used for ROI definition varied across individuals.

those as the ROI. This ROI definition procedure includes all trials (AS and PS), performances (correct and incorrect trials), and frequencies (2–60 Hz); it is therefore unbiased, age neutral, and independent with regard to our hypotheses.

Next, we averaged single-trial MNE estimates across the dipoles within each ROI. Before averaging, the sign of current fluctuations across dipoles was aligned using MNE (the "align_z" function; Gramfort et al., 2014). Neural source estimates for each ROI were then convolved with a family of complex Morelet wavelets to obtain the complex spectrum. The wavelet is described by the equation:

$$G(t,f) = \frac{1}{\sqrt{2\pi f}} \exp\left(\frac{-t^2}{2\sigma^2}\right) \exp(i2\pi f t)$$

where t is the time point within the trial epoch, f is the frequency of interest, and σ is defined as $7/2\pi f$. To obtain the power timecourses for each trial, we calculated the squared amplitude of the resulting complex spectrum. Power values were then converted to percent signal changes from baseline power (700 to 400 ms prior to the cue presentation), averaged across trials for each condition, and pooled across participants for statistical analyses. To accommodate the temporal and spectral variability across subjects (Kilner et al., 2005; Litvak et al., 2011), individual subjects' temporal-spectral estimates from each ROI were smoothed with a Gaussian smoothing kernel in both time (full-width half-maximum 40 ms) and frequency (full-width half-maximum 2 Hz).

Statistical analyses

To test for task effects (AS versus PS), age group effects (adults vs. adolescents), and task by age interactions, we performed non-parametric cluster-based permutation tests. For each ROI, we performed a mixed design two-factor analysis of variance (ANOVA) test for each time–frequency sample, where age group (adults versus adolescents) was entered as a between-subject factor, and condition (AS versus PS) was entered as a within-subject factor. *F*-statistics were then computed to assess the main effects and interaction effects. For situations where we tried to find evidence for lack of age-related or task-related differences, we calculated Jeffreys–Zellner–Siow (JZS) Bayes factor to compare evidence for competing hypotheses (Rouder et al., 2009). Briefly, band-limited power estimates were averaged across the preparatory period, and Bayes factor were calculated using with R package BayesFactor.

Controlling for multiple comparisons

To accommodate the large number of time–frequency samples being tested, we performed a cluster mass analysis to empirically determine the statistical significance and correct for multiple comparisons (Maris and Oostenveld, 2007). First we determined the uncorrected statistical threshold at $F(1,76) = 5.23$. This corresponds to an uncorrected significance threshold of $p < .05$. Then we identified temporally and spectrally continuous time–frequency samples that exceeded this uncorrected threshold. These continuous samples were then clustered into "time–frequency clusters", and we calculated the cluster statistical "mass" by summing the *F*-statistics within each cluster. We then permuted the task condition (AS and PS) and age group (adult and adolescents) labels 4000 times, recalculated the cluster mass for each randomized sample, and pooled the results to derive empirical null distributions of cluster masses. These are "null" distributions that satisfied the null hypothesis of null main effects and null interaction effects because task condition and age groups were randomly assigned for each permutation, therefore effects can only occur by chance. The proportion of values in the null distribution that was greater than the original "real", not permuted, *F*-statistic cluster mass was determined as the corrected significance value. This is the corrected cluster forming threshold we used to report all our results, and all p values were calculated based on the empirically derived null distributions. Using this approach, instead of performing a separate significance test for each time–frequency sample, we controlled for multiple comparisons by testing the significance of a single cluster mass that was computed across the entire time–frequency grid. Therefore, cluster mass tests allow for simultaneous analysis across time and frequency while inherently controlling for multiple comparisons (Maris and Oostenveld, 2007).

To further correct for the number of ROIs tested, we further corrected the cluster forming threshold using Bonferroni correction ($0.05/6 = 0.0083$; six ROIs tested: right DLPFC, right VLPFC, bilateral FEF, and bilateral IPS). For analyses that performed on the full time–frequency grid, only results that survived this stringent correction was performed (Fig. 2A, Fig. 2C, Fig. 4). For the frequency bins that showed significant main or interaction effects, we followed up with exploratory simple effect analyses of the power timecourses. For these analyses, instead of clustering *F*-statistics, we calculated cluster mass of two-sample *t*-test statistics to compare age effects for a given task condition, or paired *t*-test statistics to compare task effects for each age group. For post-hoc analyses, we presented results corrected for the number of timepoints using the same cluster mass approach. For exploratory analyses, the cluster forming threshold was determined at a threshold of $t(36) = 2.028$, $p < .025$ (two-tailed test; corrected for the number of timepoint tested, but uncorrected for the number of contrasts performed in each ROI).

Logistic regression analysis

We performed multi-level, mixed-effects logistic regressions to examine the relationship between trial-by-trial preparatory oscillatory power from each ROI and AS task performance: $P = exp.(a + bx)/(1 + exp.(a + bx))$, where P is the probability of correct AS task performance, a is the intercept term, b is the regression coefficient (slope) that quantifies the strength of the predictive effect of preparatory oscillatory power for AS task performance, and x is single-trial oscillatory power. We calculated analyses of variability by comparing variance associated with task-related oscillatory responses between age groups.

Cross-frequency coupling analysis

To assess the functional relationship between DLPFC beta-band activity and FEF alpha-band activity, we averaged power amplitude timecourses across trials for each subject, and then ran correlations between ROIs and across frequencies to assess cross-frequency amplitude coupling (Nieuwenhuis et al., 2012). We contrasted the cross-frequency coupling matrices between age groups using the randomized permutation test described above to identify coupling clusters that significantly differed between adolescents and adults. For the cluster-based permutation test, we calculated cluster mass of two-sample *t*-test statistics.

Results

Behavioral performance

We analyzed the behavioral data with a mixed-design two-way ANOVA. Accuracy (proportion of correct AS and PS trials) results revealed a significant group by condition interaction ($F(1,68) = 10.25$, $p < 0.05$, $\eta^2 = 0.072$). As expected, adults committed fewer AS errors than adolescents (adults, $M = 79.1\%$, $SD = 9.8\%$; adolescents, $M = 62.7\%$, $SD = 16.25\%$; $t(36) = 3.96$, $p < 0.01$, Cohen's $d = 0.55$), but there was no significant age-related difference for PS trials (adults, $M = 97.16\%$, $SD = 1.2\%$; adolescents, $M = 93.5\%$, $SD = 5.1$; $t(36) = 1.41$, $p = 0.084$, Cohen's $d = 0.22$). For saccade latencies, no significant main effects were found for age group ($F(1,68) = 2.49$, $p = 0.12$, $\eta^2 = 0.035$). A significant main effect was found for condition ($F(1,68) = 79.01$, $p < 0.05$, $\eta^2 = 0.53$). For both age groups, saccade latencies were faster for PS when compared to AS (PS: $M = 242$ ms, $SD =$

31 ms; AS: $M = 338$ ms, $SD = 46$ ms; $t(36) = 10.98$, $p < 0.001$, Cohen's $d = 1.81$). No developmental differences in saccade latencies for correct trials were found for either AS (adults: $M = 320$ ms, $SD = 31$ ms; adolescents: $M = 343$ ms, $SD = 65$ ms; $t(36) = -0.92$, $p = 0.18$, Cohen's $d = 0.15$) or PS (adults: $M = 235$ ms, $SD = 25$ ms; adolescents: $M = 250$ ms, $SD = 43$ ms; $t(36) = -1.45$, $p = 0.078$, Cohen's $d = 0.23$).

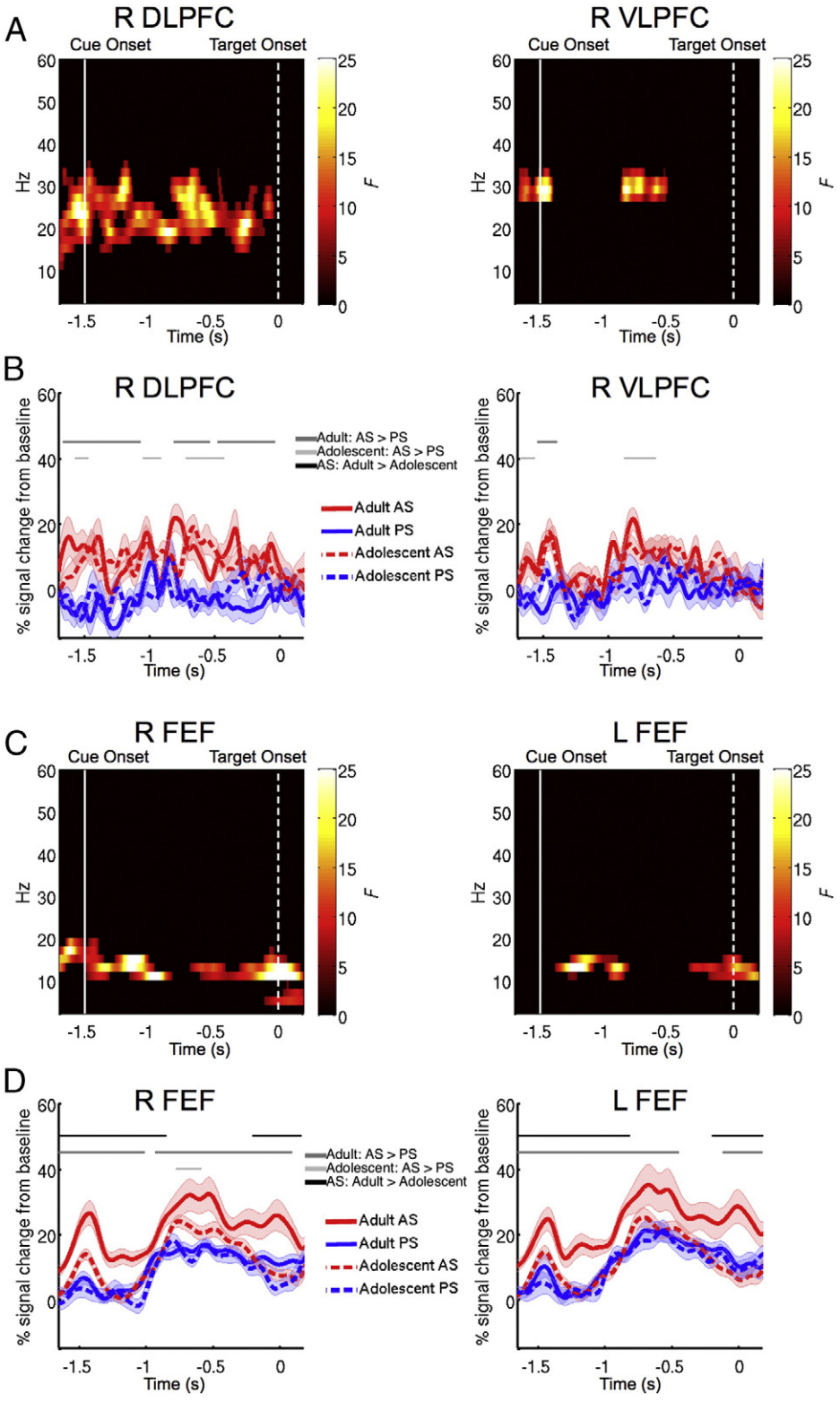

Fig. 2. (A) Time–frequency clusters in the right DLPFC and right VLPFC that showed showing significant main effects of task condition (AS vs. PS). (B) Power timecourses of right DLPFC and right VLPFC 16–36 Hz activities separated by age group and task conditions. Shaded areas represent one *SE*. Dark gray horizontal bars indicate time clusters that showed significant simple main effects in adults (AS > PS; $p < .05$, uncorrected). Light gray horizontal bars indicate significant simple main effects in adolescents (AS > PS; $p < .05$, uncorrected). (C) Time–frequency clusters in bilateral FEF that showed significant task by age interactions. (D) Power timecourses of bilateral FEF 10–18 Hz activities separated by age group and task conditions. Shaded areas represent one *SE*. Dark gray horizontal bars indicate time clusters that showed significant simple main effects in adults (AS > PS; $p < .05$, uncorrected). Light gray horizontal bars indicate significant simple main effects in adolescents (AS > PS; $p < .05$, uncorrected). Black horizontal bars indicate significant simple main effects of age for the AS task (adults > adolescents; $p < .05$, uncorrected).

Lateral PFC showed significant task effect but no age differences

We examined age group differences, task-related differences, and task by age interactions in the full time–frequency spectrum by bootstrapping statistics derived from mixed-effect two-way ANOVAs. A main effect of task was found in the right DLPFC throughout the preparatory period, specifically in the 16 to 36 Hz frequency range (Fig. 2A, < 0.001, corrected). Post-hoc analyses of simple main effects showed that for both adults and adolescents, 16 to 36 Hz power in the right DLPFC was significantly stronger for the AS task than the PS task (Fig. 2B, $p < .05$ cluster corrected). No significant developmental differences or age by task interaction was found in the right DLPFC. In the right VLPFC, two clusters showed a significant main effect of task in the 16 to 36 Hz frequency range (Fig. 2A, $p < .005$, corrected). One ranged from 176 ms before the task cue to 104 after the task cue ($p < .005$, corrected); the other one ranged from 612 ms after the task cue to 864 ms after the task cue ($p < .005$, corrected). Post-hoc tests of simple effects showed that for both adolescents and adults, during short periods of the preparatory period, 16 to 36 Hz power in the right VLPFC was significantly stronger for the AS task than for the PS task (Fig. 2B, $p < .05$ cluster corrected). No significant age group differences or age by task interaction were found in the right VLPFC. Compared to the right DLPFC, effects observed in the right VLPFC were less robust and were not sustained throughout the preparatory period. Follow up analyses focused on the right DLPFC. To follow-up on the lack of age-related differences in beta-band activity, we took a Bayesian approach and calculated the JZS Bayes factor (Rouder et al., 2009) to compare hypotheses suggesting the present or absence of age-related beta-band activity change in DLPFC. We averaged task-related changes in beta-band power for the AS task across the preparatory period, and submitted to Bayes factor analysis. Our results favored the null hypothesis, suggesting no age-related differences in beta-band activity (DLPFC: adult mean = 10.98, $SD = 4.1$; DLPFC: adolescent mean = 9.16, $SD = 5.69$, JZS Bayes factor = 2.62).

FEF showed significant age by task interaction

The right and left FEF showed a significant age by task interaction during the preparatory period in the 10–18 Hz frequency range (Fig. 2C). Specifically 10–20 Hz in the right FEF, and 10–16 Hz in the left FEF. Two significant time–frequency clusters showed this interaction effect for the right FEF, one spanned from 200 ms before task cue presentation to 644 ms into the preparatory period ($p < .005$, corrected), the other cluster ranged from 788 ms to after the target presentation ($p < .005$, corrected). For the left FEF, one cluster ranged from 96 to 620 ms after the task cue ($p < .005$, corrected), the other cluster ranged from 1216 ms after the task cue to 200 ms after the target presentation ($p < .005$, corrected). Post-hoc tests of simple effects showed that task-related modulation of 10–18 Hz power was not the same across age groups. For adults, 10–18 Hz power was significantly stronger for the AS task when compared to the PS task (Fig. 2D, $p < .05$ cluster corrected) during the preparatory period, in both the right and left FEF. However for adolescents no significant task-related modulation was found in the left FEF, and for the right FEF only a small portion of the preparatory period showed significant task difference (Fig. 2D). Further, compared to adults adolescents showed weaker 10–18 Hz power throughout the preparatory period for bilateral FEF (Fig. 2D, $p < .05$ cluster corrected). In contrast, no developmental differences in 10–19 Hz power were found for the PS task (Fig. 2D), suggesting that this task effect is specific to the AS task in our study. Consistent with our previous study we did not find significant effects in the bilateral IPS (Hwang et al., 2014).

To summarize, we observed significant task by age interactions in 10–18 Hz power in the FEF and significant task-related modulation in 16–38 Hz power in the right DLPFC and the right VLPFC. The spectral range that showed significant task effect (16–36 Hz) and task by age interaction (10–18 Hz) largely overlapped with the DLPFC beta-band (18–38 Hz) and FEF alpha-band (10–18 Hz) activities that we previously found significant task effects (Hwang et al., 2014); this frequency range is further consistent with a previous primate electrophysiology study that showed two classes of oscillatory signals each associated with enhancing task-relevant and inhibiting task-incompatible rule representation in DLPFC (Buschman et al., 2012). Henceforth, for brevity the 10–18 Hz effect will be referred to as "alpha-band activity" and the 18–38 Hz effect as "beta-band activity" hereon. Because bilateral FEF ROIs showed very similar spectral profiles, left and right FEF ROIs were then averaged before further statistical tests.

Trial-by-trial prestimulus FEF alpha-band power predicted successful saccadic inhibition

We previously found evidence suggesting that FEF alpha-band activity reflects functional inhibition of saccade generation mechanisms (Hwang et al., 2014). If preparatory alpha-band activity serves to inhibit neural activities associated with saccade initiation, it should correlate with AS task performance. That is, the stronger the alpha power the more likely this signal will inhibit saccade-related activity during the preparatory period, thus preventing an erroneous prosaccade from being generated at stimulus onset. We first investigated this relationship by performing logistic regression between trial-by-trial preparatory alpha-band power (10–18 Hz) and AS task performance. Results showed a statistically significant and positive association between preparatory FEF alpha-band power and the probability of performing a correct AS trial in adults (Fig. 3; intercept = 1.49 b = 0.0044, z = 2.91, $p < 0.005$). For adolescents, this association was not statistically significant (Fig. 3; intercept = 0.59, b = 0.0019, z = 1.92, $p = 0.078$). To test for age group differences, we included an additional age group by FEF alpha-band power interaction term into the model. The interaction term was non-significant (b = 0.0034, z = 1.60, $p = 0.11$), indicating that there were no group differences in how trial-by-trial FEF alpha-band power is associated with AS accuracy. In addition, timepoint by timepoint comparisons of signal variance (variance calculated across trials) revealed that adolescents showed higher variance in preparatory FEF alpha-band power compared to adults, but this difference did not reach statistical significance (Supplementary Fig. 1). No significant trial-by-trial brain-behavior correlations were found for other frequency bands.

To prevent reflexive saccades from being generated for the AS task, active alpha inhibition signals will have to continue beyond the preparatory period and into the initial segments of the response period, after the target location is made available. As indicated in Fig. 2 C-D, task-related difference in alpha-band power sustained beyond preparatory period. We further examined FEF evoked activities at the end of the preparatory period and before saccade initiation (Supplementary Fig. 2). We found that stimulus-evoked responses in the FEF were

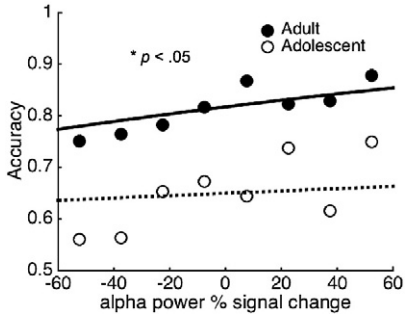

Fig. 3. (A) FEF Alpha-band power during the preparatory period predicts the probability of successfully inhibiting reflexive saccades. The solid "O" mark adults' AS task performance; the solid line is the fitted curve based on logistic regression. The hollow "O" marks adolescents' AS task performance; the dashed line is the fitted curve based on the logistic regression.

weaker for AS trials when compared to the PS task, suggesting that saccade-related processes were less active in FEF for the AS task. However this difference did not reach statistical significance after correcting for multiple comparisons for different time points.

Cross-frequency amplitude coupling

Given that the DLPFC and FEF showed task effects (AS > PS) at different frequency bands, we then investigated age-related differences in cross-frequency functional connectivity between DLPFC and FEF for the AS task. We found that for adults, there was strong amplitude coupling within the same frequency range (alpha–alpha, beta–beta) between DLPFC and FEF, as well as robust cross-frequency coupling between DLPFC beta-band activity and FEF alpha-band activity. For example there was strong coupling between DLPFC 20 Hz and FEF 10 Hz activities (Fig. 4A left panel). This pattern was less prominent in adolescents (Fig. 4A right panel). The randomization permutation test indicated that for the AS task adults showed significantly stronger coupling between DLPFC 10–26 Hz activity and FEF 10–18 Hz activity than adolescents (Fig. 4B; $p < .05$, cluster corrected). No significant differences in amplitude coupling between the FEF and the VLPFC were found when comparing tasks (AS versus PS) and age groups.

Control analyses

One common concern for developmental neuroimaging studies is that differential noise levels between age groups (i.e., head movement-related artifacts, SNR) could confound group comparison results. To exclude this possibility, we performed several control analyses. First, we compared the SNR of oscillatory power across the alpha-, beta-, and gamma-band in the V1 between adults and adolescents. Briefly, power values of each frequency were converted to SNR estimates by subtracting them from the baseline mean and dividing the difference by the baseline variance, and then averaging across frequencies and time. The V1 was chosen because our previous study found no significant age effect in this region (Velanova et al., 2008), suggesting that basic visual processes are developed by adolescence and that age-invariant activations in V1 could be used as an indication of comparable SNR between adolescents and adults. We further calculated the JZS Bayes factor to compare hypotheses suggesting the present or absence of age-related SNR differences. Evidence for both hypotheses were comparable, which suggests no, or at most very weak, effects of age-related differences in SNR (Adult mean SNR = 1.20; $SD = 0.12$; Adolescent mean SNR = 1.13; $SD = 0.11$; JZS Bayes factor = 1.49). We further inspected the post-cue and post-target evoked time-courses in both FEF and DLPFC for the AS and PS tasks, and found no significant age-related differences in evoked amplitudes. These results suggest that there are not systematic global differences that could have driven our adult versus adolescent contrasts.

An alternative interpretation is that the developmental differences in the alpha-band power we observed is not specific to cognitive control, but could instead reflect differences in the ability to sustain attention while performing hundreds of AS trials. To address this possibility, we averaged FEF alpha-band power within the preparatory period for each AS trial and compared these averaged alpha-band power between the first half and the second half of AS trials. If different levels of vigilance during the testing session influenced alpha-band power, then alpha-band power should be different between the first half and the second half of AS trials. In contrast if vigilance was not a contributing factor, then there should be no differences. To evaluate these two hypotheses, we calculated the Bayes factor for paired *t*-tests. The evidence substantially supports the null hypothesis for both age groups (adults: first half mean percent signal change in alpha-band power = 20.86, $SD = 6.99$, second half mean = 21.85, $SD = 6.03$, JZS Bayes factor = 4.075; adolescents: first half mean = 9.63, SD = 14.01, second half mean = 14.77, SD = 14.54, JZS Bayes factor = 3.25). This suggests that FEF alpha-band power was comparable between the first half and the second half of MEG testing.

Discussion

We found no age-related differences in beta-band activity between adolescents and adults, suggesting that during adolescence, DLPFC functioning is at adult levels, and may not play a critical role in the limitations in cognitive control in adolescence. This result is in agreement with previous studies indicating that prefrontal engagement during AS is adult-like by adolescence (Ordaz et al., 2013). We did however find that adolescents showed weaker functional inhibition, as indicated by decreased alpha-band power in the FEF and weaker levels of cross-frequency coupling between DLPFC and FEF, suggesting age-related limitations in the ability to communicate task-control signals for functional inhibition. Together this suggests that weaker functional inhibition of the effector system during adolescence could be related to ineffective neuronal coordination for prefrontal top-down control.

Single-unit non-human primate studies provide evidence that during the preparatory period of an AS, there is dampening of activity in regions supporting the generation of saccades. There is a decrease in the activity of saccade neurons in the FEF, which in turn could decrease excitatory inputs to the SC effectively suppressing a saccade (Johnston and Everling, 2006a; Selemon and Goldman-Rakic, 1988). This preparatory, proactive control process would prevent the oculomotor circuitry from triggering the reflexive saccade to the visual target in favor of

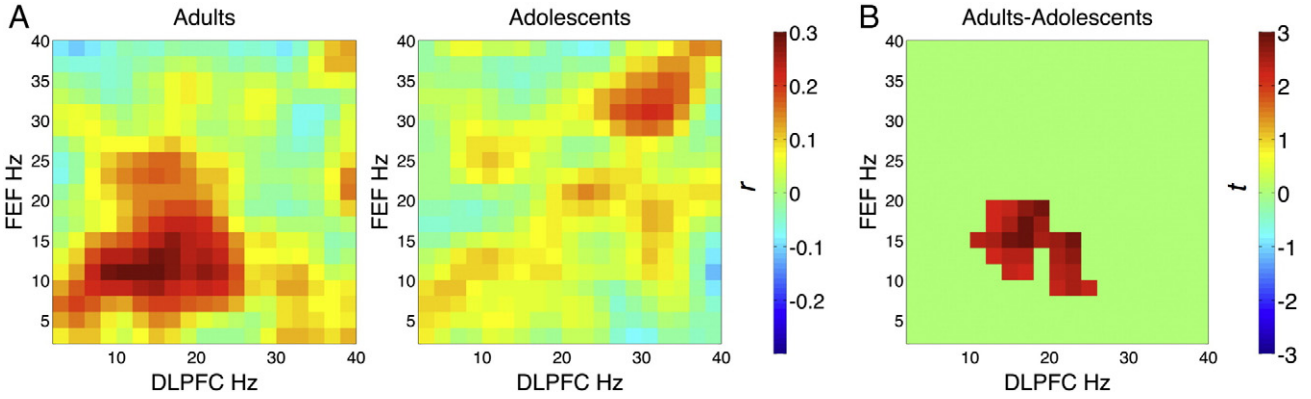

Fig. 4. Functional coupling between DLPFC beta-band activity and FEF alpha-band activity associated with the AS task. (A) Cross-frequency amplitude coupling matrices between the DLPFC and the FEF for both adults and adolescents. Colorbar indicates the strength of functional connectivity (correlation coefficient, *r*). (B) Spectral cluster that showed significant age differences. Stronger beta-alpha amplitude coupling between the DLPFC and the FEF for the AS task was found in adults (randomization test $p < .05$, cluster corrected). Colorbar indicates the test statistic *t*.

reprogramming a voluntarily antisaccade. Thus, immaturities in the processes directly related to dampening or inhibiting of neural responses related to generating motor actions may contribute to limitations in inhibitory control in adolescence. A large body of literature shows that cortical alpha-band activity serves to inhibit perceptual information (Banerjee et al., 2011; Jones et al., 2010; Kelly et al., 2010; Worden et al., 2000). Extending these findings, our previous study suggests that inhibition of preparatory saccade-related activity in the FEF is associated with increased alpha-band power (Hwang et al., 2014). In our current study, we found that, compared to adults, adolescents showed significantly weaker alpha-band power in the FEF, suggesting weaker inhibition. Together these results suggest that on a trial-by-trial basis, adolescents' FEF may not consistently sustain a neural signal that functionally inhibits preparatory saccade-related activities (Everling et al., 1998; Everling and Munoz, 2000). Weaker inhibitory signaling in the FEF may contribute to the more frequent AS errors in adolescence (Fischer et al., 1997; Klein and Foerster, 2001; Luna et al., 2004; Munoz et al., 1998). This may be due to greater variability in the timing of FEF inhibitory mechanisms. Greater variability in firing rates in adolescence has been found in orbitofrontal neurons in rodents (Sturman and Moghaddam, 2011). We found suggestive evidence for this proposal in humans, but it did not reach statistical significance.

In aggregate, our results suggest that frontal alpha-band and beta-band oscillatory dynamics supports proactive cognitive control. This is consistent with previous studies. One electroencephalography (EEG) study found that alpha-band power measured from posterior scalp electrodes (above occipital and parietal lobes) decreased in preparation for a cued saccade target (Kelly et al., 2010), which may reflect proactive deployment of attentional resources. Further, increased beta-band activity has been implicated in top-down control of goal-directed behaviors (Buschman and Miller, 2007; Gross et al., 2006; Hipp et al., 2011; Saalmann et al., 2007; Swann et al., 2009). An intracranial electrocorticography (ECOG) study reported increased beta-band power in the right PFC when patients successfully inhibited a motor response in the stop-signal task (Swann et al., 2009). This increased beta-band power could reflect the right PFC outputting control-signals to inhibit downstream motor circuitries (N.C. Swann et al., 2012). An EEG study using a modified stop-signal paradigm also found that beta-band activity to be associated with stopping of selected motor responses (Lavallee et al., 2014). A recent MEG study further showed that beta band synchrony between prefrontal and primary somatosensory cortex may act a top-down control mechanism to inhibit responses to irrelevant (non-attended) tactile stimuli (Sacchet et al., 2015).

Cross-frequency coupling has been suggested as a flexible mechanism that coordinates and integrates information processing among different brain rhythms (Canolty and Knight, 2010; Siegel et al., 2012). Here we found that for adults, there were increases in both within frequency (beta–beta, alpha–alpha) and cross-frequency beta-alpha amplitude coupling between DLPFC and FEF during correct AS trials. In our previous study, we found evidence suggesting that this coupling is initiated by DLPFC beta-band activity (Hwang et al., 2014). In contrast, both within- and cross-frequency amplitude couplings between DLPFC and FEF were reduced in adolescents. Age differences in the strength of connectivity may be associated with known developmental increases in white matter integrity in tracts supporting cortico-cortical and subcortico-cortical connectivity (Asato et al., 2010; Ashtari et al., 2007; Barnea-Goraly et al., 2005; Lebel et al., 2008; Schmithorst et al., 2002; Simmonds et al., 2014). Several potential models have suggested that the thalamus could be involved in generating alpha and beta rhythms (Bollimunta et al., 2011; Jones et al., 2009), and studies have suggested age-related changes in subcortico-cortical connectivity (Asato et al., 2010; Ferguson and Gao, 2014; Simmonds et al., 2014). Further, decreased myelination of frontal tracts (Yakovlev and Lecours, 1967) would affect the speed and validity of neuronal transmission (Stufflebeam et al., 2008), further impeding the effectiveness of task-control signaling from the DLPFC to the FEF. Our correlational analysis suggests that developmental changes in top-down connectivity and immature functional inhibition could be related. Specifically, ineffective communication of control signal from the DLPFC could result in a weaker and more variable alpha-band activity in the FEF.

There is considerable variability in the literature on defining the frequency ranges of alpha-band and beta-band oscillation. For example, beta-band activity have been defined as 13–18 Hz in some studies (Engel and Fries, 2010). It is possible that some of the effects we observed in FEF could be a combination of alpha-band and low beta-band oscillation. Our data-driven approach suggests that the 10–18 Hz task-related oscillatory signal we found in the FEF is associated with functional inhibition. Future studies that can directly manipulate oscillatory activities in local neural circuits may be able to better distinguish different contributing components in the signals we observed.

In sum, our MEG findings provide evidence suggesting that adolescents have weaker and inconsistent functional inhibition of prepotent, but task-inappropriate processes and decreased levels of inter-regional coordination. Weaker functional inhibition may result in adolescents teetering closer to a threshold of inhibitory failures and immature cognitive control. While our results are specific to oculomotor control, they provide a model for understanding the neurobiological limitations in cognitive control that could be related to more complex adolescent behaviors, such as increased impulsivity and its association with risk-taking behavior (Steinberg, 2008).

Acknowledgements

This work was supported by National Institutes of Mental Health grant R01 MH067924 and the MEG Research Seed Fund from the UPMC-Brain Mapping Center. We thank Soma Chatterji, Natalie Nawarawong, and Amanda Wright for assistance in data collection; TJ Amdurs, Anna Haridis, and Erika Taylor for technical support; and Dr. Michael Hallquist for statistical consulting.

Appendix A. Supplementary data

Supplementary data to this article can be found online at http://dx.doi.org/10.1016/j.neuroimage.2016.05.017.

References

Akaishi, R., Morishima, Y., Rajeswaren, V.P., Aoki, S., Sakai, K., 2010. Stimulation of the frontal eye field reveals persistent effective connectivity after controlled behavior. J. Neurosci. 30, 4295–4305.
Alahyane, N., Brien, D.C., Coe, B.C., Stroman, P.W., Munoz, D.P., 2014. Developmental improvements in voluntary control of behavior: effect of preparation in the fronto-parietal network? NeuroImage 98, 103–117.
Aron, A.R., 2007. The neural basis of inhibition in cognitive control. Neuroscientist 13, 214–228.
Aron, A.R., 2011. From reactive to proactive and selective control: Developing a richer model for stopping inappropriate responses. Biol. Psychiatry 69, 55–68.
Aron, A.R., Robbins, T.W., Poldrack, R.A., 2004. Inhibition and the right inferior frontal cortex. Trends Cogn. Sci. 8, 170–177.
Aron, A.R., Robbins, T.W., Poldrack, R.A., 2014. Inhibition and the right inferior frontal cortex: one decade on. Trends Cogn. Sci.
Asato, M.R., Terwilliger, R., Woo, J., Luna, B., 2010. White matter development in adolescence: a DTI study. Cereb. Cortex 20, 2122–2131.
Ashtari, M., Cervellione, K.L., Hasan, K.M., Wu, J., McIlree, C., Kester, H., Ardekani, B.A., Roofeh, D., Szeszko, P.R., Kumra, S., 2007. White matter development during late adolescence in healthy males: a cross-sectional diffusion tensor imaging study. NeuroImage 35, 501–510.
Banerjee, S., Snyder, A.C., Molholm, S., Foxe, J.J., 2011. Oscillatory alpha-band mechanisms and the deployment of spatial attention to anticipated auditory and visual target locations: supramodal or sensory-specific control mechanisms? J. Neurosci. 31, 9923–9932.
Barnea-Goraly, N., Menon, V., Eckert, M., Tamm, L., Bammer, R., Karchemskiy, A., Dant, C.C., Reiss, A.L., 2005. White matter development during childhood and adolescence: a cross-sectional diffusion tensor imaging study. Cereb. Cortex 15, 1848–1854.
Belyusar, D., Snyder, A.C., Frey, H.P., Harwood, M.R., Wallman, J., Foxe, J.J., 2013. Oscillatory alpha-band suppression mechanisms during the rapid attentional shifts required to perform an anti-saccade task. NeuroImage 65, 395–407.
Bollimunta, A., Mo, J., Schroeder, C.E., Ding, M., 2011. Neuronal mechanisms and attentional modulation of corticothalamic alpha oscillations. J. Neurosci. 31, 4935–4943.

Braver, T.S., 2012. The variable nature of cognitive control: a dual mechanisms framework. Trends Cogn. Sci. 16, 106–113.
Brown, M.R., Vilis, T., Everling, S., 2007. Frontoparietal activation with preparation for antisaccades. J. Neurophysiol. 98, 1751–1762.
Bunge, S.A., Dudukovic, N.M., Thomason, M.E., Vaidya, C.J., Gabrieli, J.D.E., 2002. Immature frontal lobe contributions to cognitive control in children: evidence from fmri. Neuron 33, 301–311.
Buschman, T.J., Miller, E.K., 2007. Top-down versus bottom-up control of attention in the prefrontal and posterior parietal cortices. Science 315, 1860–1862.
Buschman, T.J., Denovellis, E.L., Diogo, C., Bullock, D., Miller, E.K., 2012. Synchronous oscillatory neural ensembles for rules in the prefrontal cortex. Neuron 76, 838–846.
Cai, W.D., Oldenkamp, C.L., Aron, A.R., 2011. A proactive mechanism for selective suppression of response tendencies. J. Neurosci. 31, 5965–5969.
Canolty, R.T., Knight, R.T., 2010. The functional role of cross-frequency coupling. Trends Cogn. Sci. 14, 506–515.
Cohen, M.X., 2011. It's about time. Front. Hum. Neurosci. 5, 2.
Connolly, J.D., Goodale, M.A., Menon, R.S., Munoz, D.P., 2002. Human FMRI evidence for the neural correlates of preparatory set. Nat. Neurosci. 5, 1345–1352.
Dale, A.M., Fischl, B., Sereno, M.I., 1999. Cortical surface-based analysis. I. Segmentation and surface reconstruction. NeuroImage 9, 179–194.
Dale, A.M., Liu, A.K., Fischl, B.R., Buckner, R.L., Belliveau, J.W., Lewine, J.D., Halgren, E., 2000. Dynamic statistical parametric mapping: combining FMRI and MEG for high-resolution imaging of cortical activity. Neuron 26, 55–67.
Delorme, A., Makeig, S., 2004. Eeglab: an open source toolbox for analysis of single-trial eeg dynamics including independent component analysis. J. Neurosci. Methods 134, 9–21.
DeSouza, J., Menon, R., Everling, S., 2003. Preparatory set associated with pro-saccades and anti-saccades in humans investigated with event-related fmri. J. Neurophysiol. 89, 1016–1023.
Destrieux, C., Fischl, B., Dale, A., Halgren, E., 2010. Automatic parcellation of human cortical gyri and sulci using standard anatomical nomenclature. NeuroImage 53, 1–15.
Douglas, R.J., Martin, K.A., 2004. Neuronal circuits of the neocortex. Annu. Rev. Neurosci. 27, 419–451.
Durston, S., Thomas, K.M., Worden, M.S., Yang, Y., Casey, B.J., 2002. The effect of preceding context on inhibition: an event-related FMRI study. NeuroImage 16, 449–453.
Engel, A.K., Fries, P., 2010. Beta-band oscillations—signalling the status quo? Curr. Opin. Neurobiol. 20, 156–165.
Everling, S., Fischer, B., 1998. The antisaccade: a review of basic research and clinical studies. Neuropsychologia 36, 885–899.
Everling, S., Munoz, D.P., 2000. Neuronal correlates for preparatory set associated with pro-saccades and anti-saccades in the primate frontal eye field. J. Neurosci. 20, 387–400.
Everling, S., Dorris, M.C., Munoz, D.P., 1998. Reflex suppression in the anti-saccade task is dependent on prestimulus neural processes. J. Neurophysiol. 80, 1584–1589.
Everling, S., Dorris, M.C., Klein, R.M., Munoz, D.P., 1999. Role of primate superior colliculus in preparation and execution of anti-saccades and pro-saccades. J. Neurosci. 19, 2740–2754.
Ferguson, B.R., Gao, W.-J., 2014. Development of thalamocortical connections between the mediodorsal thalamus and the prefrontal cortex and its implication in cognition. Front. Hum. Neurosci. 8.
Fischer, B., Biscaldi, M., Gezeck, S., 1997. On the development of voluntary and reflexive components in human saccade generation. Brain Res. 754, 285–297.
Fischl, B., Sereno, M.I., Dale, A.M., 1999. Cortical surface-based analysis. II: Inflation, flattening, and a surface-based coordinate system. NeuroImage 9, 195–207.
Fries, P., 2015. Rhythms for cognition: communication through coherence. Neuron 88, 220–235.
Fukushima, J., Hatta, T., Fukushima, K., 2000. Development of voluntary control of saccadic eye movements. I. Age-related changes in normal children. Brain Dev. 22, 173–180.
Garavan, H., Ross, T.J., Murphy, K., Roche, R.A., Stein, E.A., 2002. Dissociable executive functions in the dynamic control of behavior: inhibition, error detection, and correction. NeuroImage 17, 1820–1829.
Gramfort, A., Luessi, M., Larson, E., Engemann, D.A., Strohmeier, D., Brodbeck, C., Parkkonen, L., Hamalainen, M.S., 2014. MNE software for processing MEG and EEG data. NeuroImage 86, 446–460.
Gross, J., Schmitz, F., Schnitzler, I., Kessler, K., Shapiro, K., Hommel, B., Schnitzler, A., 2006. Anticipatory control of long-range phase synchronization. Eur. J. Neurosci. 24, 2057–2060.
Gross, J., Baillet, S., Barnes, G.R., Henson, R.N., Hillebrand, A., Jensen, O., Jerbi, K., Litvak, V., Maess, B., Oostenveld, R., Parkkonen, L., Taylor, J.R., van Wassenhove, V., Wibral, M., Schoffelen, J.M., 2013. Good practice for conducting and reporting MEG research. NeuroImage 65, 349–363.
Haegens, S., Nacher, V., Luna, R., Romo, R., Jensen, O., 2011. Alpha-oscillations in the monkey sensorimotor network influence discrimination performance by rhythmical inhibition of neuronal spiking. Proc. Natl. Acad. Sci. U. S. A. 108, 19377–19382.
Hamalainen, M.S., Sarvas, J., 1989. Realistic conductivity geometry model of the human head for interpretation of neuromagnetic data. IEEE Trans. Biomed. Eng. 36, 165–171.
Hamalainen, M.S., Lin, F.H., Mosher, J.C., 2010. Anatomically and functionally constrained minimum-norm estimates. In: Hansen, P.C., Kringelbach, M.L., Salmelin, R. (Eds.), MEG: an introduction to methods. Oxford University Press, New York, pp. 186–215.
Handel, B.F., Haarmeier, T., Jensen, O., 2011. Alpha oscillations correlate with the successful inhibition of unattended stimuli. J. Cogn. Neurosci. 23, 2494–2502.
Hanes, D.P., Patterson, W.F., Schall, J.D., 1998. Role of frontal eye fields in countermanding saccades: visual, movement, and fixation activity. J. Neurophysiol. 79, 817–834.
Hipp, J.F., Engel, A.K., Siegel, M., 2011. Oscillatory synchronization in large-scale cortical networks predicts perception. Neuron 69, 387–396.
Hwang, K., Luna, B., 2012. The development of brain connectivity supporting prefrontal cortical functions. In: Stuss, D.T., Knight, R.T. (Eds.), Principles of Frontal Lobe Function, second ed. Oxford University Press, New York, NY.
Hwang, K., Velanova, K., Luna, B., 2010. Strengthening of top-down frontal cognitive control networks underlying the development of inhibitory control: a functional magnetic resonance imaging effective connectivity study. J. Neurosci. 30, 15535–15545.
Hwang, K., Ghuman, A.S., Manoach, D.S., Jones, S.R., Luna, B., 2014. Cortical neurodynamics of inhibitory control. J. Neurosci. 34 (29), 9551–9561.
Jensen, O., Mazaheri, A., 2010. Shaping functional architecture by oscillatory alpha activity: gating by inhibition. Front. Hum. Neurosci. 4, 186.
Johnston, K., Everling, S., 2006a. Monkey dorsolateral prefrontal cortex sends task-selective signals directly to the superior colliculus. J. Neurosci. 26, 12471–12478.
Johnston, K., Everling, S., 2006b. Neural activity in monkey prefrontal cortex is modulated by task context and behavioral instruction during delayed-match-to-sample and conditional prosaccade-antisaccade tasks. J. Cogn. Neurosci. 18, 749–765.
Jones, S.R., Pritchett, D.L., Sikora, M.A., Stufflebeam, S.M., Hamalainen, M., Moore, C.I., 2009. Quantitative analysis and biophysically realistic neural modeling of the meg mu rhythm: rhythmogenesis and modulation of sensory-evoked responses. J. Neurophysiol. 102, 3554–3572.
Jones, S.R., Kerr, C.E., Wan, Q., Pritchett, D.L., Hamalainen, M., Moore, C.I., 2010. Cued spatial attention drives functionally relevant modulation of the mu rhythm in primary somatosensory cortex. J. Neurosci. 30, 13760–13765.
Kelly, S.P., Foxe, J.J., Newman, G., Edelman, J.A., 2010. Prepare for conflict: EEG correlates of the anticipation of target competition during overt and covert shifts of visual attention. Eur. J. Neurosci. 31, 1690–1700.
Kilner, J.M., Kiebel, S.J., Friston, K.J., 2005. Applications of random field theory to electrophysiology. Neurosci. Lett. 374, 174–178.
Klein, C., Foerster, F., 2001. Development of prosaccade and antisaccade task performance in participants aged 6 to 26 years. Psychophysiology 38, 179–189.
Klimesch, W., Sauseng, P., Hanslmayr, S., 2007. EEG alpha oscillations: the inhibition-timing hypothesis. Brain Res. Rev. 53, 63–88.
Kramer, A.F., de Sather, J.C., Cassavaugh, N.D., 2005. Development of attentional and oculomotor control. Dev. Psychol. 41, 760–772.
Lavallee, C.F., Meemken, M.T., Herrmann, C.S., Huster, R.J., 2014. When holding your horses meets the deer in the headlights: time–frequency characteristics of global and selective stopping under conditions of proactive and reactive control. Front. Hum. Neurosci. 8, 994.
Lebel, C., Walker, L., Leemans, A., Phillips, L., Beaulieu, C., 2008. Microstructural maturation of the human brain from childhood to adulthood. NeuroImage 140, 1044–1055.
Lee, A.K., Hamalainen, M.S., Dyckman, K.A., Barton, J.J., Manoach, D.S., 2010. Saccadic preparation in the frontal eye field is modulated by distinct trial history effects as revealed by magnetoencephalography. Cereb. Cortex.
Litvak, V., Mattout, J., Kiebel, S., Phillips, C., Henson, R., Kilner, J., Barnes, G., Oostenveld, R., Daunizeau, J., Flandin, G., Penny, W., Friston, K., 2011. EEG and MEG data analysis in spm8. Comput. Intell. Neurosci. 2011, 852961.
Luna, B., Garver, K.E., Urban, T.A., Lazar, N.A., Sweeney, J.A., 2004. Maturation of cognitive processes from late childhood to adulthood. Child Dev. 75, 1357–1372.
Luna, B., Marek, S., Larsen, B., Tervo-Clemmens, B., Chahal, R., 2015. An integrative model of the maturation of cognitive control. Annu. Rev. Neurosci.
Maris, E., Oostenveld, R., 2007. Nonparametric statistical testing of EEG- and MEG-data. J. Neurosci. Methods 164, 177–190.
Moon, S., Barton, J., Mikulski, S., Polli, F., Cain, M., Vangel, M., Hamalainen, M., Manoach, D., 2007. Where left becomes right: a magnetoencephalographic study of sensorimotor transformation for antisaccades. NeuroImage 36, 1313–1323.
Munoz, D.P., Everling, S., 2004. Look away: the anti-saccade task and the voluntary control of eye movement. Nat. Rev. Neurosci. 5, 218–228.
Munoz, D.P., Broughton, J.R., Goldring, J.E., Armstrong, I.T., 1998. Age-related performance of human subjects on saccadic eye movement tasks. Exp. Brain Res. 121, 391–400.
Nenonen, J., Nurminen, J., Kicic, D., Bikmullina, R., Lioumis, P., Jousmaki, V., Taulu, S., Parkkonen, L., Putaala, M., Kahkonen, S., 2012. Validation of head movement correction and spatiotemporal signal space separation in magnetoencephalography. Clin. Neurophysiol. 123, 2180–2191.
Nieuwenhuis, I.L.C., Takashima, A., Oostenveld, R., McNaughton, B.L., Fernandez, G., Jensen, O., 2012. The neocortical network representing associative memory reorganizes with time in a process engaging the anterior temporal lobe. Cereb. Cortex 22, 2622–2633.
Oostenveld, R., Fries, P., Maris, E., Schoffelen, J.M., 2011. Fieldtrip: open source software for advanced analysis of MEG, EEG, and invasive electrophysiological data. Comput. Intell. Neurosci. 2011, 156869.
Ordaz, S.J., Foran, W., Velanova, K., Luna, B., 2013. Longitudinal growth curves of brain function underlying inhibitory control through adolescence. J. Neurosci. 33, 18109–18124.
Picazio, S., Veniero, D., Ponzo, V., Caltagirone, C., Gross, J., Thut, G., Koch, G., 2014. Prefrontal control over motor cortex cycles at beta frequency during movement inhibition. Curr. Biol. 24.
Ridderinkhof, K.R., van den Wildenberg, W.P., Segalowitz, S.J., Carter, C.S., 2004. Neurocognitive mechanisms of cognitive control: the role of prefrontal cortex in action selection, response inhibition, performance monitoring, and reward-based learning. Brain Cogn. 56, 129–140.
Roopun, A.K., Lebeau, F.E., Ramell, J., Cunningham, M.O., Traub, R.D., Whittington, M.A., 2010. Cholinergic neuromodulation controls directed temporal communication in neocortex in vitro. Front. Neural Circuits 4, 8.
Rouder, J.N., Speckman, P.L., Sun, D.C., Morey, R.D., Iverson, G., 2009. Bayesian t tests for accepting and rejecting the null hypothesis. Psychon. Bull. Rev. 16, 225–237.
Rubia, K., Smith, A.B., Woolley, J., Nosarti, C., Heyman, I., Taylor, E., Brammer, M., 2006. Progressive increase of frontostriatal brain activation from childhood to adulthood during event-related tasks of cognitive control. Hum. Brain Mapp. 27, 973–993.
Rubia, K., Smith, A.B., Taylor, E., Brammer, M., 2007. Linear age-correlated functional development of right inferior fronto-striato-cerebellar networks during response

inhibition and anterior cingulate during error-related processes. Hum. Brain Mapp. 28, 1163–1177.
Saalmann, Y.B., Pigarev, I.N., Vidyasagar, T.R., 2007. Neural mechanisms of visual attention: how top-down feedback highlights relevant locations. Science 316, 1612–1615.
Sacchet, M.D., LaPlante, R.A., Wan, Q., Pritchett, D.L., Lee, A.K.C., Hamalainen, M., Moore, C.I., Kerr, C.E., Jones, S.R., 2015. Attention drives synchronization of alpha and beta rhythms between right inferior frontal and primary sensory neocortex. J. Neurosci. 35, 2074–2082.
Schiller, P.H., Sandell, J.H., Maunsell, J.H., 1987. The effect of frontal eye field and superior colliculus lesions on saccadic latencies in the rhesus monkey. J. Neurophysiol. 57, 1033–1049.
Schlag-Rey, M., Amador, N., Sanchez, H., Schlag, J., 1997. Antisaccade performance predicted by neuronal activity in the supplementary eye field. Nature 390, 398–401.
Schmithorst, V.J., Wilke, M., Dardzinski, B.J., Holland, S.K., 2002. Correlation of white matter diffusivity and anisotropy with age during childhood and adolescence: a cross-sectional diffusion-tensor MR imaging study. Radiology 222, 212–218.
Selemon, L.D., Goldman-Rakic, P.S., 1988. Common cortical and subcortical targets of the dorsolateral prefrontal and posterior parietal cortices in the rhesus monkey: evidence for a distributed neural network subserving spatially guided behavior. J. Neurosci. 8, 4049–4068.
Siegel, M., Donner, T.H., Engel, A.K., 2012. Spectral fingerprints of large-scale neuronal interactions. Nat. Rev. Neurosci. 13, 121–134.
Simmonds, D.J., Hallquist, M.N., Asato, M., Luna, B., 2014. Developmental stages and sex differences of white matter and behavioral development through adolescence: a longitudinal diffusion tensor imaging (DTI) study. NeuroImage 92, 356–368.
Steinberg, L., 2008. A social neuroscience perspective on adolescent risk-taking. Dev. Rev. 28 (1), 78–106.
Stufflebeam, S., Witzel, T., Mikulski, S., Hamalainen, M., Temereanca, S., Barton, J., Tuch, D., Manoach, D., 2008. A non-invasive method to relate the timing of neural activity to white matter microstructural integrity. NeuroImage 42, 710–716.
Sturman, D.A., Moghaddam, B., 2011. Reduced neuronal inhibition and coordination of adolescent prefrontal cortex during motivated behavior. J. Neurosci. 31, 1471–1478.
Swann, N., Tandon, N., Canolty, R., Ellmore, T.M., McEvoy, L.K., Dreyer, S., DiSano, M., Aron, A.R., 2009. Intracranial eeg reveals a time- and frequency-specific role for the right inferior frontal gyrus and primary motor cortex in stopping initiated responses. J. Neurosci. 29, 12675–12685.
Swann, N., Tandon, N., Pieters, T.A., Aron, A.R., 2012a. Intracranial electroencephalography reveals different temporal profiles for dorsal- and ventro-lateral prefrontal cortex in preparing to stop action. Cereb. Cortex.
Swann, N.C., Cai, W., Conner, C.R., Pieters, T.A., Claffey, M.P., George, J.S., Aron, A.R., Tandon, N., 2012b. Roles for the pre-supplementary motor area and the right inferior frontal gyrus in stopping action: electrophysiological responses and functional and structural connectivity. NeuroImage 59, 2860–2870.
Taulu, S., Hari, R., 2009. Removal of magnetoencephalographic artifacts with temporal signal-space separation: demonstration with single-trial auditory-evoked responses. Hum. Brain Mapp. 30, 1524–1534.
Taulu, S., Kajola, M., Simola, J., 2004. Suppression of interference and artifacts by the signal space separation method. Brain Topogr. 16, 269–275.
Thut, G., Nietzel, A., Brandt, S.A., Pascual-Leone, A., 2006. Alpha-band electroencephalographic activity over occipital cortex indexes visuospatial attention bias and predicts visual target detection. J. Neurosci. 26, 9494–9502.
Uhlhaas, P.J., Roux, F., Singer, W., Haenschel, C., Sireteanu, R., Rodriguez, E., 2009. The development of neural synchrony reflects late maturation and restructuring of functional networks in humans. Proc. Natl. Acad. Sci. U. S. A. 106, 9866–9871.
Uhlhaas, P.J., Roux, F., Rodriguez, E., Rotarska-Jagiela, A., Singer, W., 2010. Neural synchrony and the development of cortical networks. Trends Cogn. Sci.
Velanova, K., Wheeler, M.E., Luna, B., 2008. Maturational changes in anterior cingulate and frontoparietal recruitment support the development of error processing and inhibitory control. Cereb. Cortex 18, 2505–2522.
Velanova, K., Wheeler, M.E., Luna, B., 2009. The maturation of task set-related activation supports late developmental improvements in inhibitory control. J. Neurosci. 29, 12558–12567.
Wehner, D., Hamalainen, M., Mody, M., Ahlfors, S., 2008. Head movements of children in MEG: quantification, effects on source estimation, and compensation. NeuroImage 40, 541–550.
Worden, M.S., Foxe, J.J., Wang, N., Simpson, G.V., 2000. Anticipatory biasing of visuospatial attention indexed by retinotopically specific alpha-band electroencephalography increases over occipital cortex. J. Neurosci. 20, 1–6.
Yakovlev, P.I., Lecours, A.-R., 1967. The myelogenetic cycles of regional maturation of the brain. Regional development of the brain in early life, pp. 3–70.
Ziegler, D.A., Pritchett, D.L., Hosseini-Varnamkhasti, P., Corkin, S., Hamalainen, M., Moore, C.I., Jones, S.R., 2010. Transformations in oscillatory activity and evoked responses in primary somatosensory cortex in middle age: a combined computational neural modeling and MEG study. NeuroImage 52, 897–912.